CHALMERS
UNIVERSITY OF TECHNOLOGY

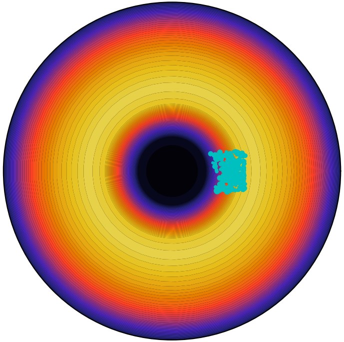

Disruption Mitigation in Tokamaks with Staggered Shattered Pellet Injection

Oskar Vallhagen

István Pusztai, Sarah Newton, Mathias Hoppe, Tünde Fülöp

Motivation

Disruption mitigation requirements:

- Uniformly radiating away thermal energy
- Control current drop by controling post-thermal quench temperature
- Avoid excessive runaway currents (high density increase)

Hard to achieve simultaneously

Motivation

Larger injections ⇒

- Faster radiative cooling, reducing localised heat loads, but...
- increase hot-tail runaway generation
- increase runaway avalanche via recombination (large D injections) [Vallhagen *et al* JPP 2020])
  - Bound electrons contribute to the target electrons, but only partially to the friction force → enhanced avalanche!

Disruption mitigation strategy

- Suggested injection scheme:
  two-stage SPI [Nardon *et al* JPP 2020]
  - stage 1: dilution cooling by large deuterium injection
  - intermediate equilibration to reduce hot-tail and conducted losses
  - stage 2: radiative cooling by neon injection
- Recombination sensitive to opacity [Vallhagen *et al* APS 2020]

Outline

- The DREAM code [Hoppe *et al* `arXiv:2103.16457`], extended with SPI model [Vallhagen MSc thesis]
  - 1D fluid-kinetic framework for disruption simulations
- Optimizing injection parameters
- Hot-tail supression with two-stage SPI
- Subsequent disruption mitigation performance
- Effect of opacity

```
                It’s time to...

* * ________   _____  ______ ___* *  ___  ___
 * \\   __   \/ __  \/  ____//   \ //   \/   \
   //  / //  / /_// /  /__ // /\  \/  / / /  /   *
  //  / //  /      /   __/// /_/  /  / / /  /   * *
_//  /_//  /  /\  \   /__//  __  /  / / /  /     *
\\________/__/ \\__\_____//_///_/__//_//__/     *
              * *          * *      *         *
     * *       *       * *      * *             *
   * * *                                 ...baby...
```

Shattered pellet injection

- Uniform distribution of speed and divergence angle
- Statistical shard size distribution with independent pellet dimensions

  [Parks GA Report 2016]
- Ablation assuming the Neutral Gas Shielding (NGS) model

  [Parks TSDW 2017]

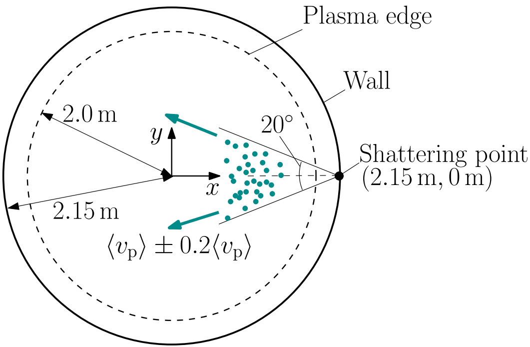

Shattered pellet injection

- Cylindrical plasma geometry
- Flux surface localised density source
- Instantaneous homogenisation and equilibration
- Varying pellet composition, speed, size and degree of shattering

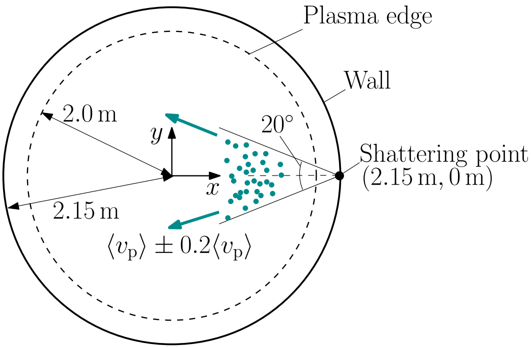

Particle and energy balance

- Time dependent ionization/recombination rate equations
- Electron energy density $W_\mathrm{M} = \frac{3}{2} n_\mathrm{M} T_\mathrm{M}$:

$$\frac{\partial W_\mathrm{M}}{\partial t} = P_\mathrm{Ohm} - P_\mathrm{line} - P_\mathrm{ioniz} + \frac{1}{r}\frac{\partial}{\partial r}\left[r D_W \frac{\partial T_\mathrm{M}}{\partial r}\right] - P_\mathrm{abl} + P_\mathrm{hot} - P_\mathrm{brems}$$

- Rechester-Rosenbluth diffusion coefficient $D_W \propto (\delta B/B)^2$
- Radiation and ionization/recombination rates from ADAS for neon and AMJUEL for hydrogen species (accounting for opacity to Lyman radiation)
  - High D density, ground state dominates $\Rightarrow$ Lyman opacity
  - Escaping fraction $\sim 10^{-3}$ under post-disruption conditions

Current evolution

- Electric field induction and diffusion
- Ohmic current with conductivity from Braams & Karney, Phys. Fluids 1989
- Hot-tail captured by kinetic equation
  - linearised, test-particle, Fokker-Planck collision operator
  - collision frequencies corrected for radiation and partial screening [Hesslow *et al* JPP 2018]
  - delta function source at $p = 0$ accounting for newly ionized electrons
  - electrons with $0 < p < p_{\mathrm{max}} = 3m_{\mathrm{e}}c$ resolved kinetically

Fluid runaway sources

$$\frac{\partial n_{\mathrm{RE}}}{\partial t} = F_p + \left(\frac{\partial n_{\text{RE}}}{\partial t}\right)^{\text{avalanche}} + \left(\frac{\partial n_{\mathrm{RE}}}{\partial t}\right)^{\mathrm{tritium}} + \left(\frac{\partial n_{\mathrm{RE}}}{\partial t}\right)^{\gamma}$$

- Flux from kinetic grid (hot-tail, Dreicer)
- Avalanche corrected for partial screening effects

  [Hesslow *et al* NF 2019]
- Tritium decay and Compton scattering (nuclear cases)

  [Fülöp *et al* JPP 2020, Martin-Solis *et al* NF 2017]

Input parameters and settings

- Initial parameters from 15 MA high-confinement ITER scenario
- $\delta B/B = 7 \cdot 10^{-4} \Rightarrow$ transport timescale $a^2/(D_W x_1^2) \sim 1$ ms, $x_1 \approx 2.4$
    - turned on when injected neon enters the plasma (single stage D+Ne or second stage Ne)
    - turned off at the end of the temperature drop – emulate re-healing flux surfaces
- $\langle v_{\mathrm{p,D}} \rangle = 800$ m/s, $\langle v_{\mathrm{p,Ne}} \rangle = 200$ m/s
- N_{s} determined by parameter scans to ensure good core penetration and assimilation

Assimilation rate deuterium injection (stage 1)

- Choose $N_{\mathrm{s,D}}$ for given N_{inj} at 97% assimilation contour (dashed green) for efficient use of pellet
- Solid green line marks core penetration

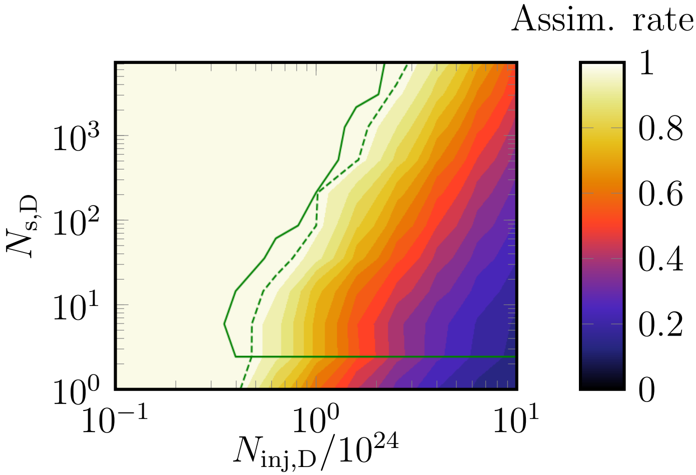

Assimilation rate neon injection (stage 2)

- Poor assimilation rate, but still enables enough radiation
- Increase in assimilation rate slows down at $N_{\mathrm{s,Ne}} \sim 50$

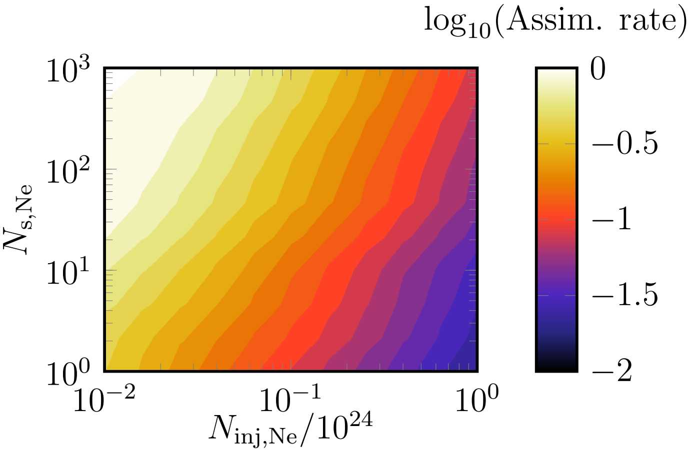

$N_{\mathrm{inj,D}} = 10^{24}$, $N_{\mathrm{s,D}} = 66$

Example: two-stage SPI

$N_{\mathrm{inj,D}} = 2 \cdot 10^{24}$, $N_{\mathrm{s,D}} = 1742$
$N_{\mathrm{inj,Ne}} = 10^{23}$, $N_{\mathrm{s,Ne}} = 50$

Example: two-stage SPI

$N_{\mathrm{inj,D}} = 2 \cdot 10^{24}$, $N_{\mathrm{s,D}} = 1742$
$N_{\mathrm{inj,Ne}} = 10^{23}$, $N_{\mathrm{s,Ne}} = 50$

Example: single-stage injection

$N_{\mathrm{inj}} = 2 \cdot 10^{24}$, $N_{\mathrm{s}} = 1742$
95% D, 5% Ne

Example: single-stage injection

$N_{\mathrm{inj}} = 2 \cdot 10^{24}$, $N_{\mathrm{s}} = 1742$
95% D, 5% Ne

Conducted thermal losses and hot-tail generation

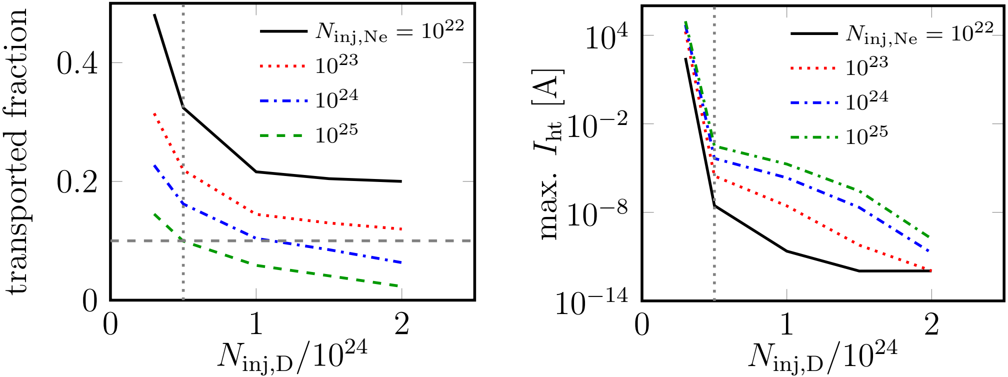

- ITER goal: transported fraction < 10% (gray dashed line) [Hollman *et al* NF 2015]
- Gray dotted line: core penetration of deuterium injection

Current quench times and runaway currents

- Current quench with fluid runaway sources added to hot-tail
- Compare non-nuclear (thin lines) and nuclear (thick lines) cases
- ITER goal: 50 (35) ms < t_{CQ} < 150 ms, $I_{\mathrm{RE}} < 0.15$ MA

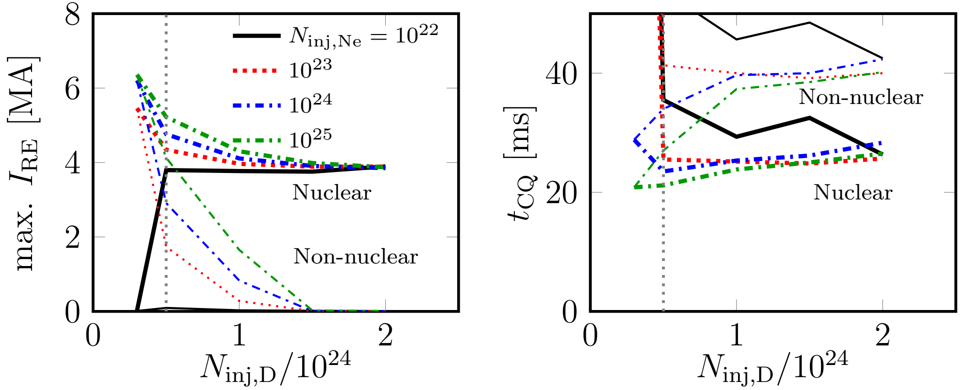

Current quench times and runaway currents w/o Ly opacity

- Higher runaway currents for large deuterium pellets
- Stronger cooling ⇒ higher E-field, more recombination ⇒ Stronger avalanche

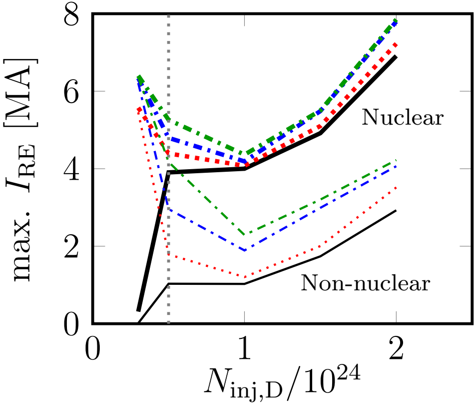

Current quench dynamics, high n_{D}

$N_{\mathrm{inj,D}} = 2 \cdot 10^{24}$, $N_{\mathrm{s,D}} = 1742$
$N_{\mathrm{inj,Ne}} = 10^{23}$, $N_{\mathrm{s,Ne}} = 50$
Transparent, from start of CQ

Energy balance in transparent and Ly-opaque limit

- Average n_{Ne}, n_{D} from case with $N_{\mathrm{inj,D}} = 2 \cdot 10^{24}$, $N_{\mathrm{inj,Ne}} = 10^{23}$
- Contributions included by AMJUEL coefficients:
  - Free-bound transitions (recombination)
  - Transitions between excited states
  - Three-body recombination
  - Population of excited states – affects ionization

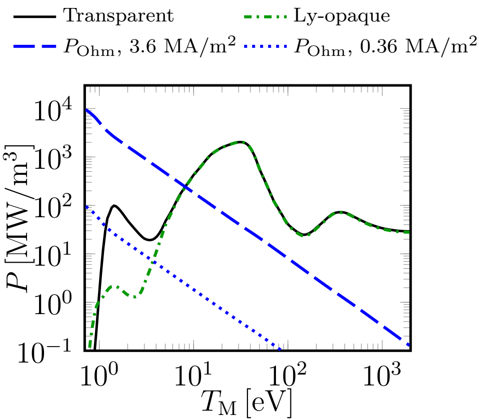

Power balance at equilibrium ionization

Summary and outlook

- The DREAM code has been extended with an SPI model
- Two-stage D/Ne injection efficiently reduces hot-tail generation
- Disruption mitigation requirements seem reachable in non-nuclear phase
- Opacity increases post-disruption temperature and postpones recombination $\Rightarrow$ decrease in avalanche
- Additional runaway supression needed in the nuclear phase

Further effects to include:

- Impact of advanced deposition models
  - Drifts
  - Ablation by fast electrons
- Realistic geometry
- MHD modeling

Material deposition

Total evolution of the charge state densities is given by

$$\frac{\partial n_{ij}}{\partial t} = \left(\frac{\partial n_{ij}}{\partial t}\right)_{\mathrm{ioniz}} + \left(\frac{\partial n_{ij}}{\partial t}\right)_{\mathrm{SPI}}. \tag{1}$$

Evolution of ion charge state densities due to ionization and recombination

$$\begin{aligned}\left(\frac{\partial n_{ij}}{\partial t}\right)_{\mathrm{ioniz}} =& (I_{i-1,j} n_{\mathrm{M}} + \langle \sigma_{\mathrm{ion},i-1,j} v \rangle) n_{i-1,j} - (I_{ij} n_{\mathrm{M}} + \langle \sigma_{\mathrm{ion},ij} v \rangle) n_{ij} + \\ & R_{i+1,j} n_{i+1,j} n_{\mathrm{M}} - R_{ij} n_{ij} n_{\mathrm{M}}.\end{aligned} \tag{2}$$

- n_{ij} is the density of charge state i of ion species j
- n_{M} is the density of the Maxwellian electron bulk

The homogenized ion density increase:

$$\left(\frac{\partial n_{ij}}{\partial t}\right)_{\mathrm{SPI}} = -f_{ij}\sum_{k=1}^{N_\mathrm{s}} \frac{4\pi r_{p,k}^2 \dot{r}_{p,k} \rho_{\mathrm{dens}} N_\mathrm{A}}{\mathcal{M}} H(r, \rho_{p,k}), \tag{3}$$

- f_{ij} particle fraction of the ablated material deposited to n_{ij} (from equilibrium)
- pellet molar mass $\mathcal{M}$
- homogenized density increase $H(r, \rho_{p,k}) = h(r, \rho_{p,k})/V'(r)$
- $h(r, \rho_{p,k})\mathrm{d}r$ fraction of the material deposited between r and $r + \mathrm{d}r$
- $V' = 4\pi^2 r R_0$ in cylindrical geometry
- Gaussian deposition kernel $h \propto \exp\left[-(r-\rho_{p,k})^2/r_{\mathrm{cld}}^2\right]$, $r_{\mathrm{cld}} \sim$ 1 cm
- computational feasibility restricts the radial resolution in the kinetic simulations: $h = \delta(r - \rho_{p,k})$

Ablation

Time derivative of the shard radii based on the updated NGS model (Parks TSDW)

$$\dot{r}_{p,k} = -\lambda(X)\left(\frac{q_{\mathrm{in}}}{q_0}\right)^{1/3}\left(\frac{\mathcal{E}_{\mathrm{in}}}{\mathcal{E}_0}\right)^{7/6}\left(\frac{r_{p,k}}{r_{p0}}\right)^{4/3}\frac{1}{4\pi r_{p,k}^2\rho_{\mathrm{dens}}}. \quad (4)$$

- solid mass density of the pellet ρ_{dens}
- $r_{p0} = 2$ mm, $q_0 = n_0\sqrt{2T_0^3/(\pi m_e)}$ and $\mathcal{E}_0 = 2T_0$, with $T_0 = 2000$ eV and $n_0 = 10^{20}$ m^{-3}
- $\lambda(X) = [27.0837 + \tan(1.48709X)]/1000\ \mathrm{kg/s}$, $X = N_{\mathrm{D}_2}/(N_{\mathrm{D}_2} + N_{\mathrm{Ne}})$
- unidirectional incident heat flux q_{in} carried by the bulk plasma electrons
- bulk electron effective energy $\mathcal{E}_{\mathrm{in}}$

Heat flux

$$q_{\mathrm{in}} = \frac{1}{4} \int m_{\mathrm{e}} c^2 (\gamma - 1) v f \, \mathrm{d}\boldsymbol{p} \tag{5}$$

- factor $1/4$ converts the isotropic heat flux to the average unidirectional heat flux facing the pellet shards

Effective energy

$$\mathcal{E}_{\mathrm{in}} = \frac{2}{n_{\mathrm{free}}} \int m_{\mathrm{e}} c^2 (\gamma - 1) f \, \mathrm{d}\boldsymbol{p}. \tag{6}$$

- $n_{\mathrm{free}} = \int f \mathrm{d}\boldsymbol{p}$
- $\mathcal{E}_{\mathrm{in}}$ reduces to $2T_{\mathrm{M}}$ for completely Maxwellian electrons

Opacity to Lyman radiation

- Opacity coefficients $B_z^j(h)$ and deexcitation rate Γ_z^j from the literature.

  [Morozov *et al* Plasma Phys. Rep. 2007, Johnson & Hinnov JQSRT 1973]
- Gives escaping fraction

$$f_{\text{esc}} = \frac{\sum_z n_z \sum_j B_z^j(h) E_z^j \Gamma_z^j}{\sum_z n_z \sum_j E_z^j \Gamma_z^j}$$

- $T_e = 1.38\,\text{eV}$, $n_\text{D} = 4 \cdot 10^{21}\,\text{m}^{-3}$, $n_{\text{e,free}} = 10^{20}\,\text{m}^{-3}$

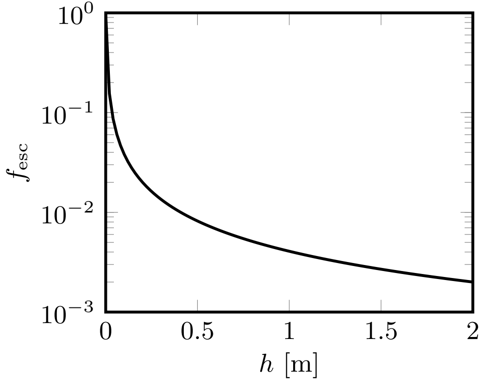

Escaping fraction f_{esc} as function of slab thickness h.

Effect of small prescribed drifts

- Shift material one radial grid cell towards LFS ($\Delta r = dr$)
- Suppresses “self-cooling” by ablated material
- Heat absorbed in pellet cloud not instantly returned to the background plasma $\Rightarrow$ account for by absorbtion term

$$\left(\frac{\partial W_{\mathrm{M}}}{\partial t}\right)_{\mathrm{abs}} = -\sum_{k=1}^{N_{\mathrm{s}}} 2 q_{\mathrm{in}} \pi r_{\mathrm{cld}}^2 H(r, \rho_{\mathrm{p},k}), \tag{7}$$

with $r_{\mathrm{cld}} \sim 1$ cm

Effect of small prescribed drifts

- Similar case as Akinobu *et al* REM 2020 ($N_{\mathrm{inj}} = 2.2 \cdot 10^{24}$, $N_{\mathrm{s}} = 300$ and $\langle v_{\mathrm{p}} \rangle = 200$ m/s)
- Shifted ⇒ no self-cooling ⇒ earlier ablation
  - Depends on cooling from absorbtion

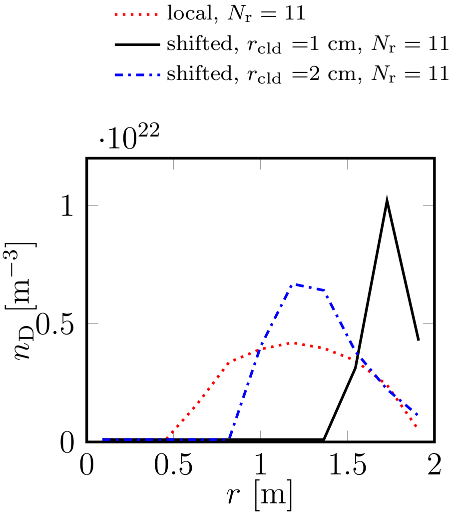

Effect of resolution and deposition kernel width

- Results insensitive to resolution
- Final profile with local deposition insensitive to r_{cld} even with higher resolution